Article

Discovery Medicine 2025; 37(203): 2978–2989
https://doi.org/10.24976/Discov.Med.202537203.249

FRZB Attenuates Ferroptosis and Oxidative Stress in Diabetic Cardiomyopathy by Modulating the AMPK/PGC-1α Signaling Pathway: A Novel Cardioprotective Mechanism

Zhangyin Zhao[1], Yinfeng Jia[1], Xuqing Hou[1,*]

[1]Department of Cardiovascular Medicine, The Second People's Hospital of Yueqing, 325608 Wenzhou, Zhejiang, China
*Correspondence: hxq108005@163.com (Xuqing Hou)
Submitted: 28 August 2025 Revised: 14 November 2025 Accepted: 25 November 2025 Published: 20 December 2025

Background: Diabetic Cardiomyopathy (DCM), a common cardiac complication in diabetic patients, is characterized by cardiac structural injury and myocardial metabolic dysfunction, ultimately leading to heart failure. Frizzled Related Protein (FRZB) contributes to the regulation of a variety of diseases, including diabetes and cardiovascular failure. However, the specific mechanism underlying its role in DCM is unclear. Therefore, this study investigated the cardioprotective role of FRZB in diabetic heart injury.

Methods: Male C57BL/6J mice were employed to construct an *in vivo* DCM mouse model using a high-fat diet combined with a streptozotocin injection. Similarly, an *in vitro* DCM model was established in H9C2 cells through high glucose (HG) exposure. Histological staining, Cell Counting Kit-8 assay, TdT-mediated dUTP Nick-End Labeling (TUNEL staining), flow cytometry, and biochemical kits were used to examine cardiac tissue morphology, cell activity, apoptosis and oxidative stress. The expression levels of ferroptosis-related indicators were quantified. Furthermore, FRZB was overexpressed or knocked down to assess its effect and determine changes in Adenosine 5′-monophosphate (AMP)-activated protein kinase (AMPK)/Peroxisome proliferator-activated receptor-γ-coactivator 1α (PGC-1α) signaling pathway-related protein levels after HG exposure.

Results: HG induced cardiomyocyte injury, ferroptosis and oxidative stress, along with downregulation of FRZB expression *in vitro* and *in vivo*. Overexpression of FRZB activated the AMPK/PGC-1α signaling pathway and significantly attenuated HG-induced oxidative stress and ferroptosis in cardiomyocytes. In contrast, silencing of FRZB effectively inhibited this pathway, exacerbating oxidative stress and ferroptosis under HG conditions. Additionally, when FRZB was overexpressed while inhibiting the AMPK/PGC-1α signaling pathway, its cardioprotective effects were abolished.

Conclusion: FRZB attenuates diabetes-induced oxidative stress and ferroptosis in cardiomyocytes by regulating the AMPK/PGC-1α signaling pathway, offering novel insights into the cardioprotective mechanisms for diabetic patients.

Keywords: diabetic cardiomyopathy; FRZB; oxidative stress; ferroptosis; AMPK/PGC-1α pathway

Introduction

Diabetic cardiomyopathy (DCM) is a distinct type of cardiomyopathy that occurs in patients with diabetes mellitus, characterized by cardiomyocyte apoptosis, ventricular dilation or hypertrophy, cardiac remodeling, myocardial ischemia, insulin resistance, and myocardial metabolic disorders [1–3]. Therefore, novel pharmacological and molecular approaches are essential to prevent ventricular dysfunction and manage myocardial metabolic dysfunction in patients with DCM.

Recent studies have linked ferroptosis to several conditions, particularly cardiovascular disease [4–6]. Ferroptosis is a type of regulated, non-apoptotic cell death induced by over-production of phospholipid hydroperoxides in an iron-dependent manner [7], which, in turn, leads to dysregulated iron metabolism, lipid peroxidation and depletion of the ferroptosis-suppressing enzyme Glutathione Peroxidase 4 (GPX4) [8,9]. Canagliflozin has been reported to alleviate myocardial oxidative stress and suppress ferroptosis in a DCM mouse model [10], indicating that inhibiting ferroptosis and oxidative stress in cardiomyocytes is crucial for treating DCM.

Adenosine 5'-monophosphate (AMP)-activated protein kinase (AMPK) is a key regulator of cellular energy metabolism and is a common therapeutic target in type 2 diabetes (T2DM) [11]. Peroxisome proliferator-activated receptor-γ-coactivator 1α (PGC-1α) is a downstream regulator of AMPK, which participates in the modulation of cellular glycolipid metabolism [12]. Numerous studies reveal that the AMPK/PGC-1α pathway is involved in reducing oxidative stress, for example, fibroblast growth factor 19 (FGF19) has been reported to reduce palmitate-induced

oxidative stress in skeletal muscle through activation of the AMPK/PGC-1α pathway [13]. Furthermore, upregulation of PGC-1α enhances mitochondrial function, prevents diabetic cardiometabolic dysfunction, and protects against diabetic cardiomyopathy [14]. Additionally, Tapan Behl *et al.* [15] summarized numerous studies showing that activating AMPK helps treat diabetes and its complications. Therefore, activation of the AMPK/PGC-1α pathway represents a crucial treatment approach to alleviate DCM.

FRZB is a member of the secretory frizzled-related protein family that is involved in regulating several diseases, including arthritis, cardiovascular conditions, and various cancers, by modulating other proteins and cell proliferation and differentiation [16–19]. This protein has been found to attenuate inflammation-induced insulin signaling dysfunction in T2DM and to be positively correlated with insulin sensitivity [20]. Studies have indicated that FRZB promotes positive effects in myocardial ischemia and heart failure, with its upregulation potentially counteracting the negative impacts on heart function under stress [21]. It is noteworthy that FRZB can reduce cardiac fibrosis and cardiac hypertrophy by suppressing oxidative stress and cardiomyocyte apoptosis [22]. These observations support FRZB as a potential therapeutic target. However, its specific protective role in DCM remains poorly investigated. Therefore, this study aims to explore the cardioprotective role of FRZB in diabetic heart injury using a DCM mouse model.

Materials and Methods

Animal Model

Male C57BL/6J mice (n = 10), aged 3 weeks and weighing 18–22 g, were acclimatized for 1 week before experiments. The mice were housed under controlled environmental conditions (temperature 22 $\pm$ 1 °C, humidity 50 $\pm$ 5%) with a 12-hour light-dark cycle and free access to food and water. Mice were randomly divided into control and high-fat diet (high glucose) groups, with 5 mice each. From 4 weeks of age, mice in the control group received a standard diet (chow), and the remaining mice were given a high-fat diet to induce a T2DM model. At 8 weeks of age, the high-fat diet-fed group received an intraperitoneal injection of STZ (30 mg/kg) to induce the T2DM model, whereas control mice were treated with an equal volume of sodium citrate buffer for three consecutive days. T2DM was confirmed on the third day after STZ injection. To minimize mice suffering, euthanasia was conducted using an overdose of anesthetic (3% pentobarbital sodium, 200 mg/Kg). After confirming the respiratory arrest, tissue samples were collected.

Hematoxylin-Eosin (H&E) and Masson's Trichrome Staining

Mouse heart tissue samples were fixed with 4% paraformaldehyde, then dehydrated, cleared, and then embedded in paraffin. Tissue sections were stained with H&E for microscopic assessment of morphological changes in myocardial tissues across different groups. Additionally, Masson's trichrome staining was performed on cardiac tissue sections to examine myocardial fibrosis.

TdT-mediated dUTP Nick-End Labeling (TUNEL)

Cardiac tissues were sectioned into 4 µm slices, washed with phosphate-buffered saline (PBS), and permeabilized with 0.3% Triton X-100. Apoptotic cells were stained using a TUNEL fluorescein isothiocyanate (FITC) Apoptosis Detection Kit and counterstained with 4',6-diamidino-2-phenylindole, following the manufacturer's instructions (G1502 and G1012, Servicebio, Wuhan, China). TUNEL-positive cells were visualized and assessed using a fluorescence microscope (APX100, Olympus, Tokyo, Japan).

Real-time Quantitative Polymerase Chain Reaction (RT-qPCR)

Total RNA was extracted using TRIzol® reagent (DP424, TIANGEN, Beijing, China). The cDNA was synthesized using the Maxima First Strand cDNA Synthesis Kit (K1641, Thermo Fisher, Waltham, MA, USA). RT-qPCR was performed using SYBR® Premix EX TaqTM (RR390Q, Takara Dalian, China). Primers used in RT-qPCR are listed in Table 1. Relative mRNA expression levels were calculated using the $2^{-\Delta\Delta Ct}$ method, with β-actin serving as the internal control.

Western Blot (WB) Analysis

Total protein was extracted from H9C2 cells using RIPA lysis buffer (P0013B, Beyotime, Shanghai, China). An equal amount of protein (30 µg per sample) was resolved by electrophoresis and subsequently transferred onto PVDF membranes. The membranes were blocked for 1 hour and then incubated overnight at 4 °C with the following primary antibodies: anti-FRZB (ab273582; 1:1000; Abcam), anti-GPX4 (ab125066; 1:1000; Abcam), anti-ACSL4 (ab155282; 1:1000; Abcam), anti-Ferritin (ab74973; 1:1000; Abcam), anti-Solute Carrier Family 7 Member 11 (SLC7A11) (HA600098; 1:1000; HUABIO), anti-AMPK (ET1608-40; 1:1000; HUABIO), anti-p-AMPK (ET1701-37; 1:1000; HUABIO), and anti-PGC-1α (A12348; 1:1000; Abclonal). The following day, membranes were washed with PBST and incubated for 30 minutes at 37 °C with horseradish peroxidase-conjugated Goat Anti-Rabbit IgG H&L secondary antibody (1:5000; ab96899; Abcam). Protein bands were visualized using an enhanced chemiluminescence kit (BL520b, Biosharp Life Science, Anhui, China), and images were captured with

Table 1. A list of primers used in RT-qPCR.

Primer	Sequences
Frizzled Related Protein (FRZB)	Forward: 5′-GAGGAGCTGCCAGTGTACGAC-3′ Reverse: 5′-GAAAATCAGCTCCGTCCG C-3′
Acyl-CoA synthetase long-chain family member 4 (ACSL4)	Forward: 5′-CTTCCTCTTAAGGCCGGGAC3′ Reverse: 5′-TCTCTTTGCCATAGCGTTTTTAG-3′
Prostaglandin-endoperoxide synthase 2 (PTGS2)	Forward: 5′-TGAGTACCGCAAACGCTTCT3′ Reverse: 5′-CAGCCATTTCCTTCTCTCCTGT-3′
β-actin	Forward: 5′-ACTATTGGCAACGAGCGGTTCC-3′ Reverse: 5′-GCACTGTGTTGGCATAGAGGT-3′

a chemiluminescence system (Tanon-4600, Yuanpinghao Biotechnology Co., Ltd., Beijing, China).

Cell Culture

The rat cardiomyocyte cell line (H9C2 Cells, GNR 5) was obtained from the Cell Bank of the Chinese Academy of Sciences (Shanghai, China) and authenticated by STR analysis and mycoplasma testing. Cells were cultured in DMEM (11320033, Gibco, USA) containing 10% fetal bovine serum (A5670701, Gibco, USA) and 1% streptomycin/penicillin. For the high-glucose (HG) group, the culture medium was supplemented with 25 mM glucose and 0.2 mM palmitic acid (PAL, Sigma, USA). In contrast, the control group cells were cultured in medium containing 5 mM glucose. Both groups were incubated for 48 hours before transfection. At 24 hours post-transfection, H9C2 were treated with 10 µM dorsomorphin (Compound C, S7840, Selleck, TX, USA) for 60 minutes at 37 °C.

FRZB Overexpression (OE) and Knockdown (sh)

Based on previous protocol [23], the overexpression construct was generated by PCR cloning of FRZB into the pcDNA3.1 vector (Sino Biological), with the empty vector serving as the control, and transfected using Lipofectamine®2000. For the knockdown construct, FRZB-shRNA was inserted into pSilencer 4.1 (Shanghai Sangon Biotech), with the scramble shRNA vector serving as the negative control, and the construct was packaged and purified using the lentiviral system. The cell transfection was performed following the manufacturer's instructions. Lentivirus transduction was conducted at a multiplicity of infection (MOI) of 5. After 48 hours of incubation, puromycin (60210ES25, Asen Corporation, Shanghai, China) was added to select stable cell lines. Overexpression and knockdown efficiency are presented in the **Supplementary materials**.

Cell Viability

Cell viability was determined using the Cell Counting Kit-8 (CCK-8). H9C2 cells were exposed to 25 mM glucose and 0.2 mM palmitic acid for 24, 48, or 72 hours. After treatment, 10 µL of CCK-8 solution was added to each well, and the plates were incubated at 37 °C for 2 hours. Subsequently, absorbance (OD) was measured according to standard procedure using a microplate reader (CMax Plus, Shanghai, China). Cell viability was calculated as follows:

Cell viability (%) = $[(OD_{HG\ group} - OD_{blank}) / (OD_{control\ group} - OD_{blank})] \times 100\%$.

Where "blank wells" contain only culture medium and CCK-8 reagent, and were used to eliminate background absorption.

Flow Cytometry

Cell suspensions were prepared from each group to assess HG-induced apoptosis in H9C2 cells. Apoptosis was evaluated using flow cytometry with the Annexin V-FITC/PI apoptosis kit (LIANKE BIO, Hangzhou, China), following the manufacturer's instruction. The cell suspension was adjusted to a concentration of 1×10^5/mL, after which 10 µL of PI was added, and the cells were incubated at room temperature for 15 minutes in the dark. Finally, apoptosis was quantified using a CytoFLEX flow cytometer (BECKMAN, USA).

Evaluation of Reactive Oxygen Species (ROS) Levels

Intracellular ROS levels in H9C2 cells were assessed using a Reactive Oxygen Species Assay Kit (CA1410, Solarbio, Beijing, China). Cells were incubated with 2',7'-dichlorodihydrofluorescein diacetate (DCFH-DA) under controlled experimental conditions at 37 °C for 20 minutes. After incubation, the cells were washed three times and then examined under an inverted fluorescence microscope (CKX53, OLYMPUS, Japan) to determine fluorescence intensity.

Assessment of Oxidative Stress Level

After 24 hours of incubation under HG conditions, the cell pellets were collected. Subsequently, 1 mL of extraction buffer was added to each pellet, followed by ultrasonic homogenization. The lysates were then centrifuged, and the supernatant was obtained for further analysis. Intracellular levels of lactate dehydrogenase (LDH), malondialdehyde (MDA), and glutathione (GSH) were determined using the LDH Content Assay Kit (BC0685), MDA Content Assay

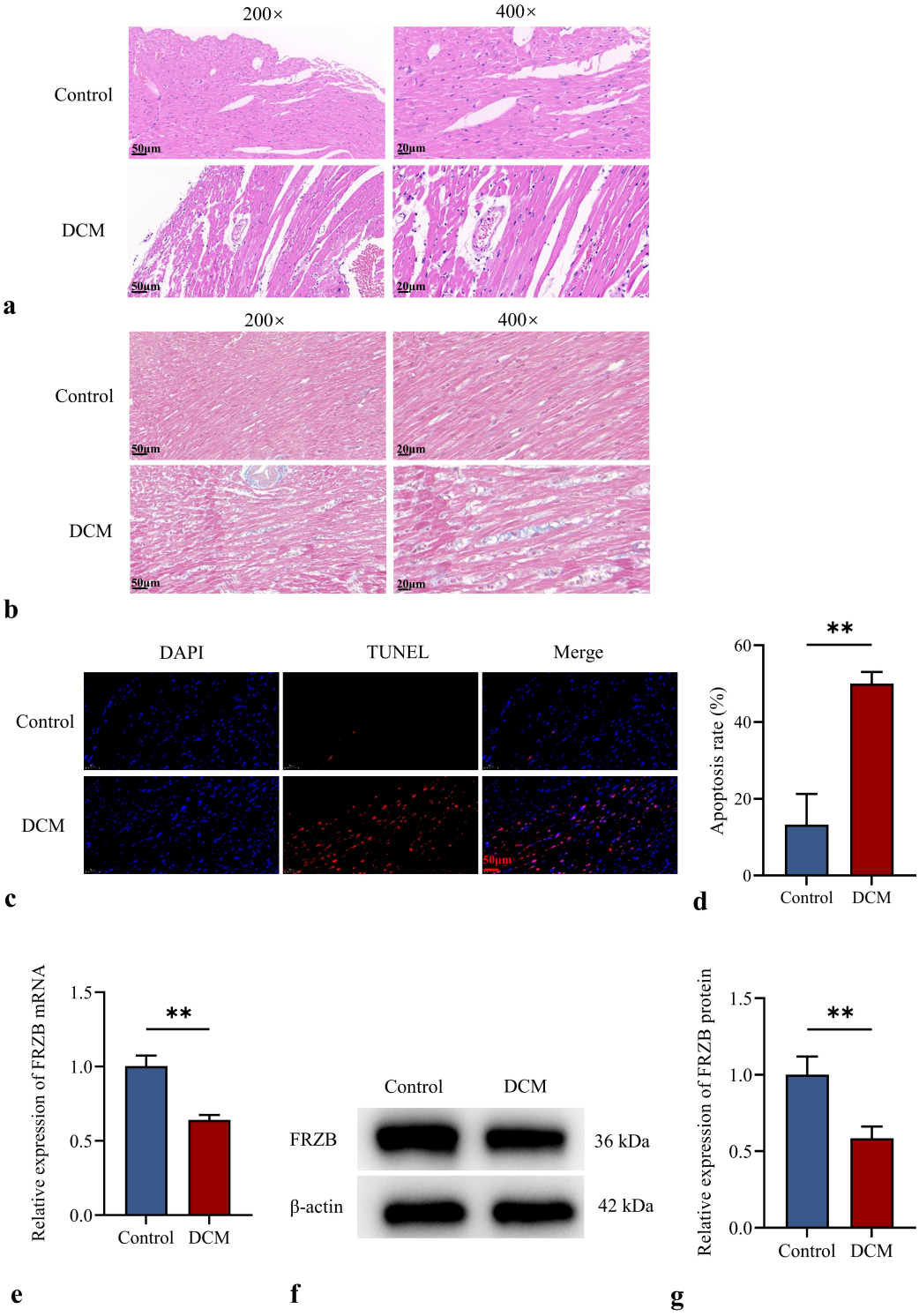

Fig. 1. Myocardial damage and FRZB downregulation in DCM mice. (a,b) Myocardial tissue morphology was assessed using H&E and Masson's trichrome staining (scale bar: 50 μm, magnification, 200× and scale bar: 20 μm, magnification, 400×). (c,d) The proportion of apoptotic cells was assessed using a TUNEL assay (scale bar: 50 μm, magnification, 200×). (e) The relative expression levels of FRZB using RT-qPCR in the control and DCM groups. (f,g) WB analysis of FRZB in the control and DCM groups. n = 5; $^{**}p < 0.01$. FRZB, Frizzled Related Protein; DCM, Diabetic Cardiomyopathy; H&E, Hematoxylin-Eosin; TUNEL, TdT-mediated dUTP Nick-End Labeling; WB, Western Blot.

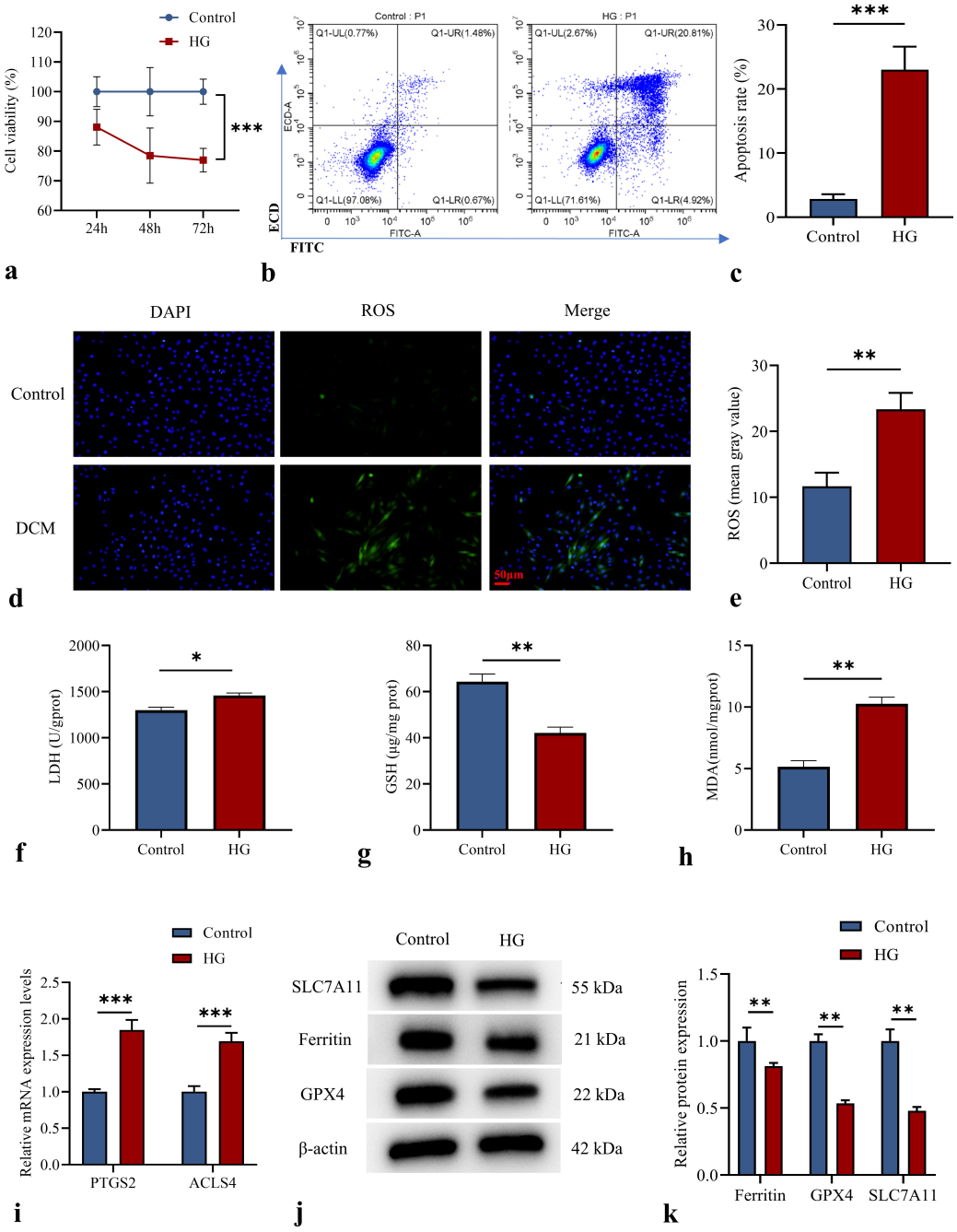

Fig. 2. HG induces oxidative stress and ferroptosis in cardiomyocytes. (a) Cell viability was evaluated at 24, 48, and 72 hours using the CCK-8 assay. (b,c) Apoptotic cell proportions were analyzed via flow cytometry. (d,e) ROS levels were measured using a fluorescent staining assay (scale bar: 50 μm, magnification: 200×). (f–h) The levels of LDH, GSH and MDA were assessed using biochemical assays. (i) The relative expression levels of PTGS2 and ACSL4 were determined using RT-qPCR. (j,k) WB analysis of SLC7A11, GPX4 and ferritin. n = 6; *$p < 0.05$, **$p < 0.01$, ***$p < 0.001$. HG, high glucose; CCK-8, Cell Counting Kit-8; ROS, Reactive Oxygen Species; LDH, lactate dehydrogenase; MDA, malondialdehyde; GSH, glutathione; PTGS2, Prostaglandin-endoperoxide synthase 2; ACSL4, Acyl-CoA synthetase long-chain family member 4; SLC7A11, Solute Carrier Family 7 Member 11; GPX4, Glutathione Peroxidase 4.

Kit (BC0025), and GSH Content Assay Kit (BC1175), respectively (Solarbio, Beijing, China).

Statistical Analyses

Statistical analysis was conducted using GraphPad Prism version 9.0 (GraphPad Prism Inc., San Diego, CA, USA). The findings are expressed as the mean ± standard deviation. Differences between groups were determined using *T*-tests or one-way analysis of variance (ANOVA), followed by Tukey's post hoc test where appropriate. Statistical significance was defined at a *p*-value of less than 0.05.

Results

Myocardium Was Significantly Damaged and FRZB Was Downregulated in DCM Mice

To evaluate the pathological changes in the cardiac muscle in DCM mice, a DCM mouse model was developed using a high-fat diet combined with STZ injection. Histological staining showed well-organized structure, with evenly sized cell nuclei and minimal collagen fiber deposition in the control group. In contrast, myocardial tissues from the DCM group revealed a disorganized structure, irregular nucleus size, and significant collagen accumulation (Fig. 1a,b). TUNEL staining showed a substantially higher proportion of apoptotic cells in the DCM group compared with the control group ($p < 0.01$, Fig. 1c,d), indicating structural damage in the myocardium of DCM mice. Moreover, FRZB expression was significantly downregulated in the DCM group compared to the control group ($p < 0.01$, Fig. 1e–g).

HG Induces Oxidative Stress and Ferroptosis in Cardiomyocytes

To explore the effect of HG on H9C2 cardiomyocytes, cell viability was assessed at 24, 48, and 72 hours post HG treatment. As depicted in Fig. 2a, cell viability decreased at 72 hours ($p < 0.001$). Flow cytometry analysis revealed an increase in the proportion of apoptotic cells in the HG group ($p < 0.001$, Fig. 2b,c).

Furthermore, ROS analysis demonstrated a significant increase in intracellular ROS in HG-treated H9C2 cardiomyocytes ($p < 0.01$, Fig. 2d,e). Similarly, biochemical assay results indicated that the level of the cytotoxic marker LDH ($p < 0.05$) and the lipid peroxidation marker MDA ($p < 0.01$) significantly increased, while the antioxidant GSH levels decreased ($p < 0.05$, Fig. 2f–h) in the HG group, reflecting oxidative stress in HG-treated cells.

Additionally, RT-qPCR analysis showed that mRNA expression of ferroptosis-related markers PTGS2 and ACSL4 was substantially increased in the HG group ($p < 0.001$, Fig. 2i). WB analysis showed that the levels of the ferroptosis-related protective factors SLC7A11, GPX4, and ferritin were significantly decreased in the HG group ($p < 0.01$, Fig. 2j,k).

FRZB Expression Is Downregulated in HG-induced Cardiomyocytes

Given that FRZB contributes to the regulation of diabetes and cardiovascular diseases and is associated with oxidative stress, this study evaluated its expression in DCM. FRZB levels were quantified in the HG-treated cardiomyocytes using RT-qPCR and WB analyses. As illustrated in Fig. 3a–c, the expression of FRZB was significantly downregulated under HG conditions, indicating that FRZB may act as a potential regulator in DCM.

FRZB Overexpression Attenuates HG-induced Oxidative Stress and Ferroptosis in Cardiomyocytes

To elucidate the specific role of FRZB in DCM, FRZB was overexpressed in cardiomyocytes, and its upregulation was confirmed in the experimental group using RT-qPCR and WB analyses (Fig. 4a–c). ROS analysis showed a significant decline in ROS levels after FRZB overexpression ($p < 0.01$, Fig. 4d,e). Biochemical assays further indicated that FRZB overexpression enhanced the antioxidant response, as evidenced by elevated GSH levels ($p < 0.05$) and reduced LDH and MDA levels ($p < 0.05$, Fig. 4f–h). Similarly, RT-qPCR demonstrated a notable decrease in the mRNA levels of the ferroptosis markers PTGS2 and ACSL4 in the HG-oe-FRZB group ($p < 0.001$, Fig. 4i).

WB analysis of ferroptosis-related proteins showed a substantial increase in ferroptosis inhibitors in the HG-oe-FRZB group ($p < 0.01$, Fig. 4j,k), confirming that ferroptosis was inhibited. These findings indicate that overexpression of FRZB significantly attenuates HG-induced oxidative stress and ferroptosis in cardiomyocytes. Furthermore, WB analysis of the AMPK/PGC-1α pathway components showed a significant increase in p-AMPK/t-AMPK and PGC-1α protein levels ($p < 0.001$, Fig. 4l,m), indicating activation of the AMPK/PGC-1α signaling pathway.

FRZB Knockdown Exacerbates HG-Induced Oxidative Stress and Ferroptosis in Cardiomyocytes

To further clarify the role of FRZB in HG-induced oxidative stress and ferroptosis in cardiomyocytes, a FRZB knockdown cell model was established, and reduced FRZB expression was confirmed in the experimental group compared to the control group (Fig. 5a–c). In the HG-sh-FRZB group, ROS levels were considerably increased ($p < 0.01$, Fig. 5d,e), and GSH levels were decreased ($p < 0.01$), whereas LDH and MDA levels were substantially elevated ($p < 0.05$, Fig. 5f–h). RT-qPCR analysis revealed an upregulation of the ferroptosis markers PTGS2 and ACSL4 ($p < 0.001$, Fig. 5i). Furthermore, WB analysis showed that the levels of ferroptosis inhibitors SLC7A11, GPX4, and ferritin were significantly decreased ($p < 0.05$, Fig. 5j,k). Additionally, analysis of the AMPK/PGC-1α pathway revealed a pronounced reduction in the phosphorylated-to-total AMPK ratio and in PGC-1α protein levels ($p < 0.01$,

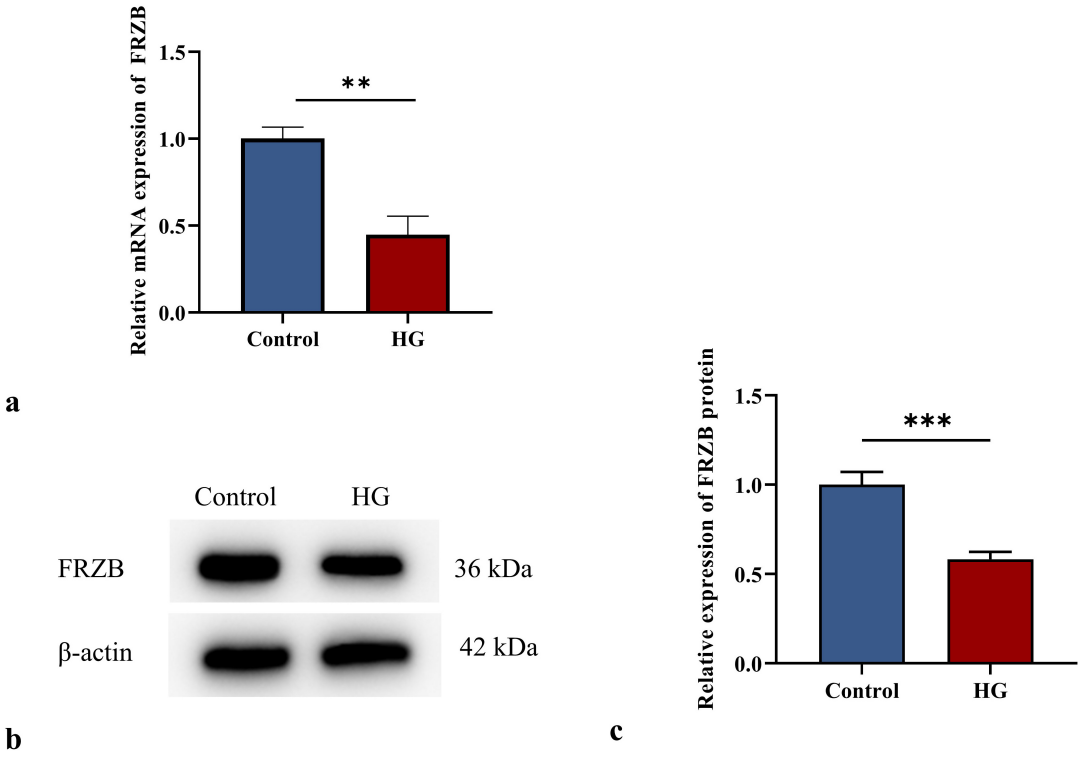

Fig. 3. FRZB expression is downregulated in HG-induced cardiomyocytes. (a) The mRNA expression levels of FRZB using RT-qPCR. (b,c) The protein expression levels of FRZB using WB analysis. n = 6; $^{**}p < 0.01$, $^{***}p < 0.001$.

Fig. 5l,m), indicating that the activity of the AMPK/PGC-1α signaling pathway was notably diminished under these conditions.

Inhibition of the AMPK/PGC-1α Signaling Pathway Reverses the Protective Effects of FRZB on Cardiomyocytes

To further elucidate the critical role of the AMPK/PGC-1α pathway in FRZB-mediated cardioprotection, AMPK was pharmacologically inhibited with Compound C in HG-oe-FRZB cardiomyocytes. As illustrated in Fig. 6a,b, Compound C markedly reduced AMPK phosphorylation and PGC-1α expression ($p < 0.01$), confirming effective pathway inhibition. Notably, this inhibition reversed the antioxidant effects of FRZB overexpression, as evidenced by a significant decrease in GSH levels ($p < 0.01$) and increases in LDH and MDA concentrations ($p < 0.001$, Fig. 6c–e). WB analysis further revealed a coordinated downregulation of the ferroptosis-suppressing proteins SLC7A11, GPX4, and ferritin ($p < 0.01$, Fig. 6f,g). Crucially, Compound C treatment completely abolished FRZB's cytoprotective effects, leading to aggravated ferroptosis and exacerbated oxidative stress.

Collectively, these pharmacological interventions provide compelling evidence that activation of the AMPK/PGC-1α pathway is an essential mechanism underlying FRZB's cardioprotective effects in diabetic cardiomyopathy and highlights its key role in mitigating diabetic cardiac injury.

Discussion

DCM is a leading cause of heart failure in diabetic patients. Current treatment methods primarily focus on blood glucose control, lipid reduction, and increased physical activity; however, there are still no effective medications or treatment strategies that directly repair damaged myocardial tissue. Hence, it is crucial to investigate pathogenic mechanisms and identify novel protective strategies. In this study, we identified that oxidative stress and ferroptosis are prominent characteristics of DCM and found that FRZB alleviates diabetic cardiomyopathy by targeting ferroptosis and oxidative stress via activation of the AMPK/PCG1α signaling pathway.

Consistent with previous studies, HG exposure induces structural damage, ferroptosis, oxidative stress, and apoptosis in cardiomyocytes [24,25]. In our study, H9C2 cardiomyocytes treated with HG exhibited decreased cell viability, increased apoptosis rates, enhanced oxidative stress, and elevated ferroptosis-related markers. Furthermore, WB and RT-qPCR analyses indicated that FRZB expression was significantly reduced compared to the control group. To investigate the role of FRZB, we overexpressed the FRZB gene *in vitro* and found that HG-induced

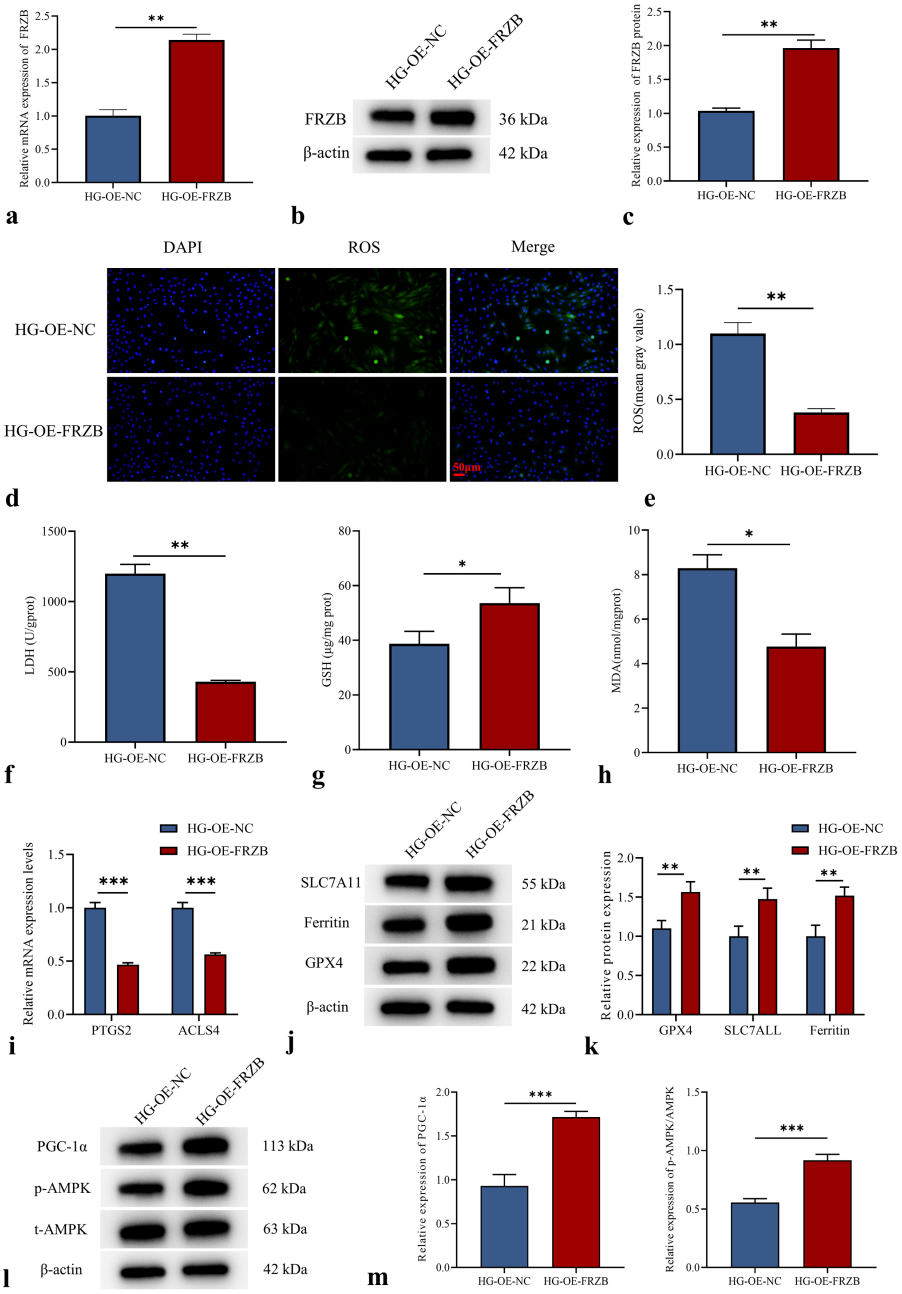

Fig. 4. Overexpression of FRZB attenuates HG-induced oxidative stress and ferroptosis in cardiomyocytes. (a) The relative expression levels of FRZB using RT-qPCR after overexpression. (b,c) WB analysis of FRZB after overexpression. (d,e) The levels of ROS using the Reactive Oxygen Species Assay Kit after FRZB overexpression (scale bar: 50 μm, magnification, 200×). (f–h) The levels of LDH, GSH and MDA were measured by biochemical assay after FRZB overexpression. (i) The expression levels of ferroptosis markers PTGS2 and ACSL4 using RT-qPCR after FRZB overexpression. (j,k) WB analysis of SLC7A11, GPX4, and ferritin after FRZB overexpression. (l,m) WB analysis of p-AMPK, t-AMPK, and PGC-1α after FRZB overexpression. n = 6; *$p < 0.05$, **$p < 0.01$, ***$p < 0.001$. AMPK, Adenosine 5'-monophosphate (AMP)-activated protein kinase; PGC-1α, Peroxisome proliferator-activated receptor-γ-coactivator 1α.

oxidative stress and ferroptosis were significantly alleviated in cardiomyocytes. Conversely, FRZB knockdown exacerbated oxidative stress and ferroptosis under HG conditions. Similarly, inhibition of oxidative stress and ferroptosis has been reported to mitigate HG-induced cardiomyocyte injury [26], and improving myocardial oxidative stress, restoring mitochondrial integrity, and inhibiting ferroptosis can alleviate the functional impairment and pathological changes in DCM [10]. Moreover, FRZB has been shown to inhibit the Wnt/β-catenin signaling path-

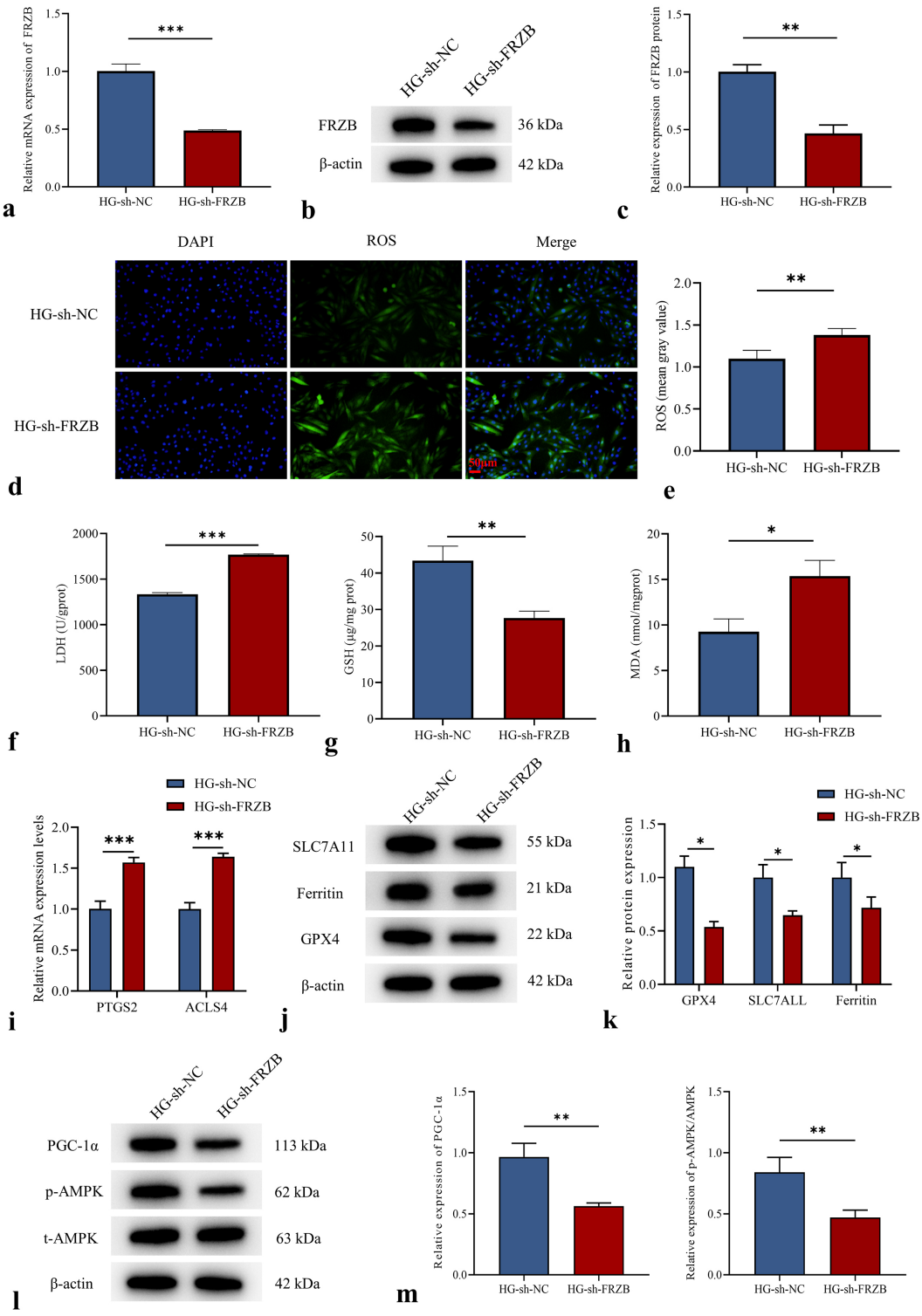

Fig. 5. FRZB knockdown exacerbates HG-induced oxidative stress and ferroptosis in cardiomyocytes. (a) The relative expression levels of FRZB after knockdown using RT-qPCR. (b,c) WB analysis of FRZB after knockdown. (d,e) The levels of ROS by Reactive Oxygen Species Assay Kit after FRZB knockdown (scale bar: 50 μm, magnification, 200×). (f–h) The levels of LDH, GSH and MDA were measured by biochemical assays after FRZB knockdown. (i) The relative expression levels of ferroptosis-related markers PTGS2 and ACSL4 after FRZB knockdown using RT-qPCR. (j,k) WB analysis of SLC7A11, GPX4, and ferritin after FRZB knockdown. (l,m) WB analysis of p-AMPK, t-AMPK, and PGC-1α after FRZB knockdown. n = 6; *$p < 0.05$, **$p < 0.01$, ***$p < 0.001$.

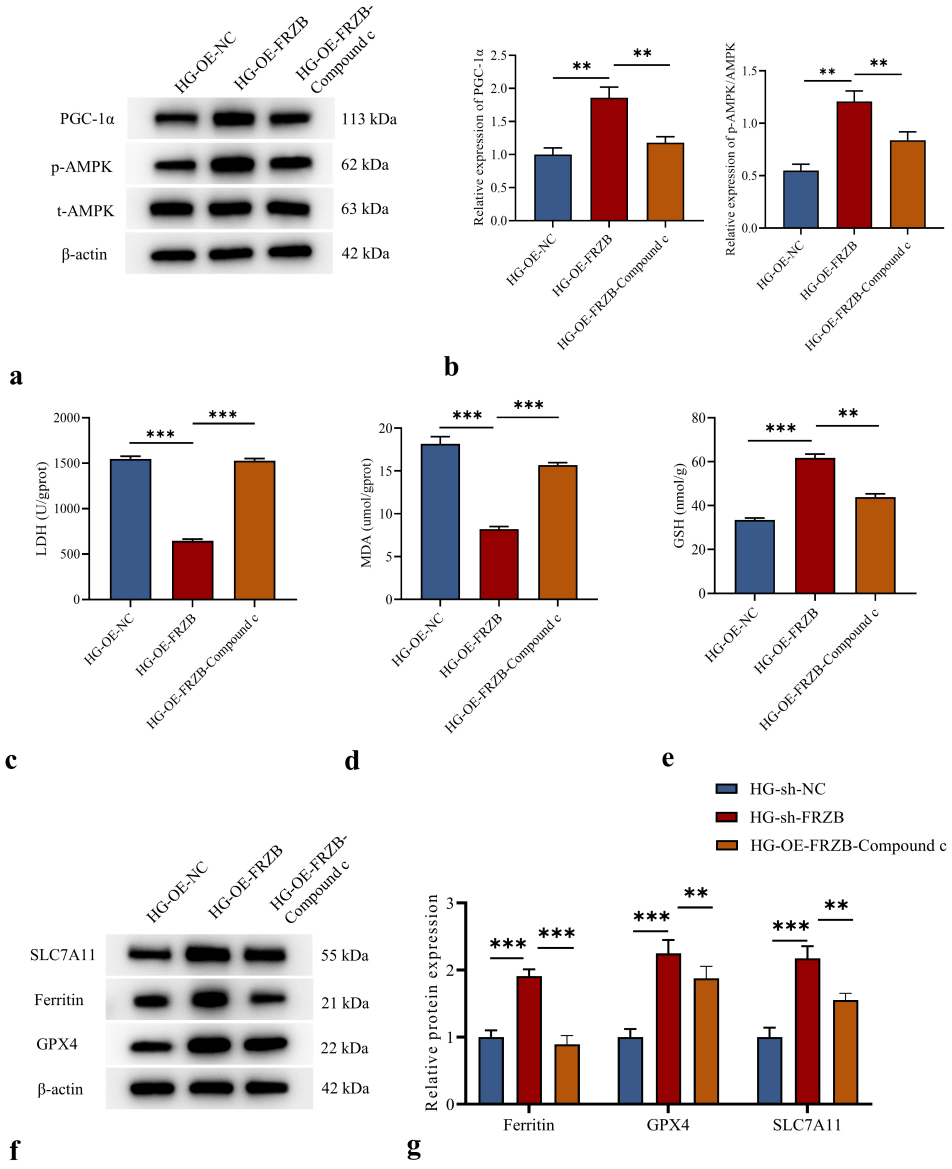

Fig. 6. Inhibition of the AMPK/PGC-1α signaling pathway reverses the protective effects of FRZB on cardiomyocytes. (a,b) WB analysis of p-AMPK, t-AMPK, and PGC-1α. (c–e) LDH, MDA, and GSH levels were determined by biochemical assays. (f,g) WB analysis of SLC7A11, GPX4, and ferritin protein. n = 6; **$p < 0.01$, ***$p < 0.001$.

way, thereby reducing abnormal proliferation, migration, and mitochondrial fission of cardiac fibroblasts [27]. These findings highlight the key role of FRZB in the protection and treatment of DCM.

However, the specific mechanism by which FRZB regulates diabetic cardiomyopathy remains unknown. Zhang *et al*. [28] found that activating the AMPK pathway can inhibit lipid peroxidation and ferroptosis, thereby reducing lipotoxicity in cardiomyocytes. Wang *et al*. [29] further reported that sulforaphane (SFN) activates nuclear factor erythroid 2-related factor 2 through AMPK, and increases ferritin and SLC7A11 levels, thereby inhibiting ferroptosis and DCM-related pathological processes. In a mouse model of DCM, pharmacological activation of AMPK has been reported to improve energy metabolism disorders caused by impaired glucose uptake, thereby reducing T2DM-induced cardiac injury [30]. In addition, evidence indicates that the AMPK/PGC-1α pathway plays a crucial role in diabetes [31–33], and we speculate that some interaction between FRZB and the AMPK/PGC-1α pathway.

As a member of the frizzled-related protein family, FRZB belongs to a group of proteins whose regulatory relationship with the AMPK pathway has been described in several studies. For instance, in the glycolipid-rich environment associated with diabetic cardiomyopathy, SFRP2 can regulate downstream PGC1-α and its related pathways by activating the phosphorylation of AMPK [18]. In

myocardial infarction (MI) and hypoxia-related myocardial injury models, SFRP5 promotes phosphorylation of AMPK at Thr172 site (upregulating the expression of p-AMPK^Thr172 protein), thereby improving mitochondrial function and reducing cardiomyocyte apoptosis, inflammation, and oxidative stress, and ultimately exerting cardioprotective effects [34]. In our study, overexpression and knockdown of FRZB resulted in activation or inhibition of the AMPK/PGC-1α pathway, respectively, indicating that FRZB alleviates diabetic cardiomyopathy by positively regulating the AMPK/PGC-1α signaling pathway. Furthermore, when FRZB was overexpressed while the AMPK/PGC-1α pathway was inhibited, its protective effects on cardiomyocytes were abolished, further validating this mechanism. Although direct protein-protein interactions between the members of the frizzled-related proteins and AMPK/PGC-1α have not been completely defined, current evidence suggests that FRZB and related family members likely act through indirect upstream signaling, with AMPK activation serving as a key downstream, dependence-mediating mechanism.

Our findings show that FRZB ameliorates oxidative stress and ferroptosis in DCM by activating the AMPK/PGC-1α signaling axis. While our findings strongly support the mechanistic link between FRZB and pathway activation, whether FRZB directly modulates AMPK/PGC-1α or acts via upstream regulatory mechanisms remains unclear, warranting further molecular investigation. Despite several valuable insights, this study has two critical limitations: (1) the absence of clinical validation using patient-derived samples, and (2) the reliance on in vitro cellular models without in vivo confirmation. Future investigations should prioritize translational validation using preclinical animal models and human tissue analyses to strengthen the clinical relevance of these findings.

Conclusion

In conclusion, FRZB mitigates diabetes-induced ferroptosis and oxidative stress in cardiomyocytes by regulating the AMPK/PGC-1α signaling pathway. The findings uncover a previously unknown protective mechanism of FRZB in DCM, providing a promising therapeutic target for treating diabetes-related cardiomyopathy and other cardiovascular diseases.

Availability of Data and Materials

The data and materials that support the findings of this study are available from the corresponding author upon reasonable request.

Author Contributions

ZZ: Conceptualization, formal analysis, methodology and writing-original draft. YJ: Methodology, formal analysis, data curation, supervision. and writing-original draft. XH: Investigation, methodology, writing-original draft. All authors contributed to important editorial changes in the manuscript. All authors read and approved the final manuscript. All authors have participated sufficiently in the work and agreed to be accountable for all aspects of the work.

Ethics Approval and Consent to Participate

All animal experiments were approved by the Animal Ethics Committee of South Zhejiang Institute of Radiation Medicine and Nuclear Technology Applications (ZFY20250305). All procedures were carried out in accordance with institutional ethical guidelines, with efforts made to minimize animal use and suffering.

Acknowledgment

Not applicable.

Funding

This research received no external funding.

Conflict of Interest

The authors declare no conflict of interest.

Supplementary Material

Supplementary material associated with this article can be found, in the online version, at https://doi.org/10.24976/Discov.Med.202537203.249.

References

[1] Zhao X, Liu S, Wang X, Chen Y, Pang P, Yang Q, *et al*. Diabetic cardiomyopathy: Clinical phenotype and practice. Frontiers in Endocrinology. 2022; 13: 1032268. https://doi.org/10.3389/fendo.2022.1032268.

[2] Dillmann WH. Diabetic Cardiomyopathy. Circulation Research. 2019; 124: 1160–1162. https://doi.org/10.1161/CIRCRESAHA.118.314665.

[3] Nakamura K, Miyoshi T, Yoshida M, Akagi S, Saito Y, Ejiri K, *et al*. Pathophysiology and Treatment of Diabetic Cardiomyopathy and Heart Failure in Patients with Diabetes Mellitus. International Journal of Molecular Sciences. 2022; 23: 3587. https://doi.org/10.3390/ijms23073587.

[4] Fang X, Ardehali H, Min J, Wang F. The molecular and metabolic landscape of iron and ferroptosis in cardiovascular disease. Nature Reviews. Cardiology. 2023; 20: 7–23. https://doi.org/10.1038/s41569-022-00735-4.

[5] Galy B, Conrad M, Muckenthaler M. Mechanisms controlling cellular and systemic iron homeostasis. Nature Reviews. Molecular Cell Biology. 2024; 25: 133–155. https://doi.org/10.1038/s41580-023-00648-1.

[6] Lin X, Xin L, Meng X, Chen D. Vaspin inhibits ferroptosis: A new hope for treating myocardial ischemia-reperfusion injury. CytoJournal. 2024; 21: 64. https://doi.org/10.25259/Cytojournal_141_2024.

[7] Dixon SJ, Lemberg KM, Lamprecht MR, Skouta R, Zaitsev EM, Gleason CE, *et al*. Ferroptosis: an iron-dependent form

of nonapoptotic cell death. Cell. 2012; 149: 1060–1072. https://doi.org/10.1016/j.cell.2012.03.042.

[8] Cui C, Yang F, Li Q. Post-Translational Modification of GPX4 is a Promising Target for Treating Ferroptosis-Related Diseases. Frontiers in Molecular Biosciences. 2022; 9: 901565. https://doi.org/10.3389/fmolb.2022.901565.

[9] Stockwell BR. Ferroptosis turns 10: Emerging mechanisms, physiological functions, and therapeutic applications. Cell. 2022; 185: 2401–2421. https://doi.org/10.1016/j.cell.2022.06.003.

[10] Du S, Shi H, Xiong L, Wang P, Shi Y. Canagliflozin mitigates ferroptosis and improves myocardial oxidative stress in mice with diabetic cardiomyopathy. Frontiers in Endocrinology. 2022; 13: 1011669. https://doi.org/10.3389/fendo.2022.1011669.

[11] Carling D. AMPK signalling in health and disease. Current Opinion in Cell Biology. 2017; 45: 31–37. https://doi.org/10.1016/j.ceb.2017.01.005.

[12] Abu Shelbayeh O, Arroum T, Morris S, Busch KB. PGC-1α Is a Master Regulator of Mitochondrial Lifecycle and ROS Stress Response. Antioxidants (Basel, Switzerland). 2023; 12: 1075. https://doi.org/10.3390/antiox12051075.

[13] Guo A, Li K, Xiao Q. Fibroblast growth factor 19 alleviates palmitic acid-induced mitochondrial dysfunction and oxidative stress via the AMPK/PGC-1α pathway in skeletal muscle. Biochemical and Biophysical Research Communications. 2020; 526: 1069–1076. https://doi.org/10.1016/j.bbrc.2020.04.002.

[14] Xu W, Wang Y, Guo Y, Liu J, Ma L, Cao W, *et al*. Fibroblast growth factor 19 improves cardiac function and mitochondrial energy homoeostasis in the diabetic heart. Biochemical and Biophysical Research Communications. 2018; 505: 242–248. https://doi.org/10.1016/j.bbrc.2018.09.046.

[15] Behl T, Gupta A, Sehgal A, Sharma S, Singh S, Sharma N, *et al*. A spotlight on underlying the mechanism of AMPK in diabetes complications. Inflammation Research. 2021; 70: 939–957. https://doi.org/10.1007/s00011-021-01488-5.

[16] Guan H, Zhang J, Luan J, Xu H, Huang Z, Yu Q, *et al*. Secreted Frizzled Related Proteins in Cardiovascular and Metabolic Diseases. Frontiers in Endocrinology. 2021; 12: 712217. https://doi.org/10.3389/fendo.2021.712217.

[17] Tong S, Ji Q, Du Y, Zhu X, Zhu C, Zhou Y. Sfrp5/Wnt Pathway: A Protective Regulatory System in Atherosclerotic Cardiovascular Disease. Journal of Interferon & Cytokine Research: the Official Journal of the International Society for Interferon and Cytokine Research. 2019; 39: 472–482. https://doi.org/10.1089/jir.2018.0154.

[18] Ma T, Huang X, Zheng H, Huang G, Li W, Liu X, *et al*. SFRP2 Improves Mitochondrial Dynamics and Mitochondrial Biogenesis, Oxidative Stress, and Apoptosis in Diabetic Cardiomyopathy. Oxidative Medicine and Cellular Longevity. 2021; 2021: 9265016. https://doi.org/10.1155/2021/9265016.

[19] Liu J, Zheng X, Zhang C, Zhang C, Bu P. Lcz696 Alleviates Myocardial Fibrosis After Myocardial Infarction Through the sFRP-1/Wnt/β-Catenin Signaling Pathway. Frontiers in Pharmacology. 2021; 12: 724147. https://doi.org/10.3389/fphar.2021.724147.

[20] Pachori AS, Madan M, Nunez Lopez YO, Yi F, Meyer C, Seyhan AA. Reduced skeletal muscle secreted frizzled-related protein 3 is associated with inflammation and insulin resistance. Obesity (Silver Spring, Md.). 2017; 25: 697–703. https://doi.org/10.1002/oby.21787.

[21] Vatner DE, Zhang J, Zhao X, Yan L, Kudej R, Vatner SF. Secreted frizzled protein 3 is a novel cardioprotective mechanism unique to the clinically relevant fourth window of ischemic preconditioning. American Journal of Physiology. Heart and Circulatory Physiology. 2021; 320: H798–H804. https://doi.org/10.1152/ajpheart.00849.2020.

[22] Gu Y, Ding Y, Zhang X, Li Y, Shang Z. Secreted frizzled-related protein 3 alleviated cardiac remodeling induced by angiotensin II via inhibiting oxidative stress and apoptosis in mice. European Journal of Pharmacology. 2022; 934: 175303. https://doi.org/10.1016/j.ejphar.2022.175303.

[23] Li X, Pang W, Fan H, Wang H, Zhang L. FRZB affects *Staphylococcus* aureus induced osteomyelitis in human bone marrow derived stem cells by regulating the Wnt/β catenin signaling pathway. Experimental and Therapeutic Medicine. 2023; 26: 531. https://doi.org/10.3892/etm.2023.12230.

[24] Tian H, Huang Q, Cheng J, Xiong Y, Xia Z. Rev-erbα attenuates diabetic myocardial injury through regulation of ferroptosis. Cellular Signalling. 2024; 114: 111006. https://doi.org/10.1016/j.cellsig.2023.111006.

[25] Puhari SSM, Yuvaraj S, Vasudevan V, Ramprasath T, Rajkumar P, Arunkumar K, *et al*. Isolation and characterization of fucoidan from four brown algae and study of the cardioprotective effect of fucoidan from Sargassum wightii against high glucose-induced oxidative stress in H9c2 cardiomyoblast cells. Journal of Food Biochemistry. 2022; 46: e14412. https://doi.org/10.1111/jfbc.14412.

[26] Li F, Hu Z, Huang Y, Zhan H. Dexmedetomidine ameliorates diabetic cardiomyopathy by inhibiting ferroptosis through the Nrf2/GPX4 pathway. Journal of Cardiothoracic Surgery. 2023; 18: 223. https://doi.org/10.1186/s13019-023-02300-7.

[27] Jiang SX, Zhou ZY, Tu B, Song K, Lin LC, Liu ZY, *et al*. Epigenetic regulation of mitochondrial fission and cardiac fibrosis via sFRP3 promoter methylation. Cellular and Molecular Life Sciences: CMLS. 2024; 81: 483. https://doi.org/10.1007/s00018-024-05516-5.

[28] Zhang W, Lu J, Wang Y, Sun P, Gao T, Xu N, *et al*. Canagliflozin Attenuates Lipotoxicity in Cardiomyocytes by Inhibiting Inflammation and Ferroptosis through Activating AMPK Pathway. International Journal of Molecular Sciences. 2023; 24: 858. https://doi.org/10.3390/ijms24010858.

[29] Wang X, Chen X, Zhou W, Men H, Bao T, Sun Y, *et al*. Ferroptosis is essential for diabetic cardiomyopathy and is prevented by sulforaphane *via* AMPK/NRF2 pathways. Acta Pharmaceutica Sinica. B. 2022; 12: 708–722. https://doi.org/10.1016/j.apsb.2021.10.005.

[30] Wang W, Wang Z, Meng Z, Jiang S, Liu Z, Zhu HY, *et al*. Platycodin D Ameliorates Type 2 Diabetes-Induced Myocardial Injury by Activating the AMPK Signaling Pathway. Journal of Agricultural and Food Chemistry. 2024; 72: 10339–10354. https://doi.org/10.1021/acs.jafc.3c07311.

[31] Li N, Zhu QX, Li GZ, Wang T, Zhou H. Empagliflozin ameliorates diabetic cardiomyopathy probably *via* activating AMPK/PGC-1α and inhibiting the RhoA/ROCK pathway. World Journal of Diabetes. 2023; 14: 1862–1876. https://doi.org/10.4239/wjd.v14.i12.1862.

[32] Yu Y, Jia YY, Li HJ. Sodium butyrate improves mitochondrial function and kidney tissue injury in diabetic kidney disease via the AMPK/PGC-1α pathway. Renal Failure. 2023; 45: 2287129. https://doi.org/10.1080/0886022X.2023.2287129.

[33] Cao R, Tian H, Zhang Y, Liu G, Xu H, Rao G, *et al*. Signaling pathways and intervention for therapy of type 2 diabetes mellitus. MedComm. 2023; 4: e283. https://doi.org/10.1002/mco2.283.

[34] Huang X, Yan Y, Zheng W, Ma Y, Wang X, Gong W, *et al*. Secreted Frizzled-Related Protein 5 Protects Against Cardiac Rupture and Improves Cardiac Function Through Inhibiting Mitochondrial Dysfunction. Frontiers in Cardiovascular Medicine. 2021; 8: 682409. https://doi.org/10.3389/fcvm.2021.682409.